RSC Advances

PAPER

View Article Online
View Journal | View Issue

Cite this: *RSC Adv.*, 2022, **12**, 30928

Pyridine ionic liquid functionalized bimetallic MOF solid-phase extraction coupled with high performance liquid chromatography for separation/analysis sunset yellow

Jun Wu, Shuyu Wan, Ouwen Xu, Hanyang Song, Jing Yang and Xiashi Zhu *

Received 22nd September 2022
Accepted 21st October 2022

DOI: 10.1039/d2ra05980k

rsc.li/rsc-advances

An effective method based on the pyridine ionic liquid functionalized bimetallic MOF solid-phase extractant (Cu/Co-MOF@[PrPy][Br]) coupled with high performance liquid chromatography (HPLC) for the separation/analysis sunset yellow was established. Cu/Co-MOF@[PrPy][Br] was characterized by FTIR, XRD, SEM and TEM. Several important factors, such as pH, amount of extractant, extract time, and types of eluents were investigated in detail. Under the optimal conditions, linear range of the method was 0.05–40.00 μg mL^{-1}, the detection limit was 0.02 μg mL^{-1}, and the linear correlation was good (R^2 = 0.9992). The analysis of sunset yellow in soda, effervescent tablet and jelly proved that the method was simple and effective.

1 Introduction

Dyes (natural dyes, synthetic dyes) are used in food industry due to their advantages of stability, uniform color and low cost in food processing.[1] Sunset yellow as a food additive[2] provided the desired color and appearance, and is also commonly used in cosmetics and pharmaceuticals.[3] The overuse of this dye and its release into the environment and water through associated industry effluents cause environmental pollution and the spread of various diseases, including allergic and asthmatic reactions, liver cell damage, DNA damage, and potential immunotoxicity and reproductive toxics.[4] Therefore, it is necessary to establish a sensitive, accurate and effective method for the detection of sunset yellow in real samples.

The determination methods of sunset yellow include UV-visible spectrophotometry,[5] high performance liquid chromatography,[6] electrochemical analysis[7] and fluorescence spectrometry.[8] Due to the complex composition of the real sample and the low content of sunset yellow, liquid phase extraction and solid phase extraction are often used to pretreat the sample.[9] Solid phase extraction (SPE) concentrates, separates and purifies samples by means of selective adsorption and selective elution. Compared with liquid phase extraction, SPE has the advantages of strong selectivity, high recovery, less solvent and simple operation.[10]

The selection of extractant is crucial in SPE. Initially-at first, the materials include activated carbon,[11] SiO_2,[12] graphene,[13] metal organic framework material,[14] covalent organic framework material.[15] With the deepening of the research, the existing functionalization of SPE extractant, such as magnesium hydroxide/carbon nanotube composite,[16] ionic liquid functionalized silica,[17] magnetic cyclodextrin modified graphene oxide,[18] ionic liquid modified metal organic framework material[19] could further improve the performance of SPE, expand the application range of the solid phase extraction technology.

Metal organic framework (MOF) is porous structures constructed from the coordinative bonding between organic linkers and metal ions.[20] It has unique pore space, large specific surface area. Functionalization of MOF means to change the properties of materials by replacing metal ions,[21] changing the organic ligands[22] and introducing other components[23] with MOF as the main body, so that the types of MOF are greatly enriched. In recent years, some metal organic framework functionalized with graphene oxide,[24] magnetic nanoparticles,[25] multi-walled carbon nanotubes,[26] chitosan[27] and ionic liquids[28] have been widely used in solid-phase extraction. Ionic liquids (ILs) are liquid molten salts at temperature below 100 °C which generally consist of organic cations and inorganic or organic anions. Due to their outstanding characteristics, its have achieved lots of successful applications.[19] Studies have shown that ILs functionalized MOF composites (MOF@ILs) integrate the advantages of MOF and ILs, it can be used as solid-phase extraction agents, enabling the further development of solid-phase extraction technology. There have been related reports on the use of MOF@ILs composites for solid-phase extraction,[29,30] but there is no report on the use of pyridinium ionic liquid-functionalized bimetallic MOF composites for the separation and enrichment of sunset yellow.

College of Chemistry and Chemical Engineering, College of Guangling, Yangzhou University, Yangzhou, 225002, China. E-mail: xszhu@yzu.edu.cn; Fax: +86-514-87975244; Tel: +86-514-87975244

In this experiment, Cu/Co-MOF@[PrPy][Br] composites were prepared and was as solid-phase extractant coupled with high-performance liquid chromatography for the separation and analysis sunset yellow. The Cu/Co-MOF@[PrPy][Br] composites combine the advantages of ILs and MOF, resulting in greatly improved extraction performance. The method is simple and effective for the determination of sunset yellow in real sample.

2 Experimental

2.1 Instruments and reagents

SH-C constant temperature oscillator, vacuum drying oven (Shanghai Yiheng Scientific Instrument Co., Ltd), Shimadzu high performance liquid chromatograph (Shimadzu Technology Co., Ltd), Mettler Toledo pH meter (Shanghai Jingke Lei Magnetic), Fourier transform infrared spectrometer (Bruker, Germany), Centrifuge TDL80-2B (Shanghai Anting Scientific Instrument Factory).

Cupric nitrate, *N*,*N*-dimethylformamide (DMF), ethanol, methanol, acetone, acetonitrile, cobalt nitrate hexahydrate, trimesic acid, pyridine, *n*-butane bromide and sunset yellow are analytical grade, and acetonitrile is HPLC grade. The above reagents were purchased from Sinopharm Chemical Reagent Co., Ltd.

Sunset yellow stock solution: 10.0 μg mL^{-1}.

Buffer solution: 0.1 mol/L HAc/NaAc, 0.1 mol/L $NH_3 \cdot H_2O$/NH_4Cl.

2.2 Preparation of [PrPy][Br]

0.08 mol of pyridine and equimolar of bromoethane were added to a 100 mL three-necked flask with a reflux condenser, and stirred at 80 °C for 6 hours. After the reaction, it was washed three times with ethyl acetate and finally the obtained product was vacuum-dried at 70 °C for 12 hours to obtain [PrPy][Br].[31]

2.3 Preparation of Cu/Co-MOF

Weight 1.42 g copper nitrate trihydrate, 0.73 g cobalt nitrate hexahydrate and 1.00 g trimesic acid were added to the mixed solution containing 17.00 mL H_2O, 17.00 mL DMF and 17.00 mL ethanol, and poured into the reactor after ultrasonication for 30 minutes. The hydrothermal reaction was carried out at 85 °C for 20 hours. After the reaction, it was washed with ethanol, and finally the obtained product was vacuum-dried at 60 °C for 12 hours to obtain Cu/Co-MOF.[32]

2.4 Preparation of Cu/Co-MOF@[PrPy][Br]

Added 0.50 g [PrPy][Br] to a small sealed beaker with 40.00 mL of acetone and stirred for an hour, then added 1.50 g Cu/Co-MOF and stirred in air to completely evaporate the acetone. After the acetone was completely removed, the product was washed with absolute ethanol, and finally placed in a vacuum drying oven at 60 °C for 12 hours to obtain Cu/Co-MOF@[PrPy][Br].[33]

2.5 Extraction and elution process

Added appropriate amount of sunset yellow (1.0 μg mL^{-1} standard solution or real sample solution) and 2.00 mL of pH 5.0 buffer solution to the centrifuge tube, dilute to 10.00 mL, accurately weigh 5.00 mg of the composite material, and shake at 25 °C for 15 minutes. Centrifuge, decant the supernatant, add 3.00 mL of methanol, and shake at 25 °C for 10 minutes. After centrifugation, the supernatant was decanted and measured by Shimadzu high performance liquid chromatograph.

2.6 Sample handling

Soda: take 20.00 mL of carbonated beverages in a beaker, degassed by ultrasonic, then filter with a 0.22 μm filter to remove particulate matter in the sample, and store it in a 50 mL centrifuge tube for determination.

Effervescent tablet: take one effervescent tablet (3.70 g) in a small beaker, add 10.00 mL of distilled water to dissolve, filter it with a 0.22 μm filter head, and store it in a 50 mL centrifuge tube for determination.

Jelly: take 2.00 g of jelly in a beaker, add 10.00 mL of distilled water, heat it in a water bath at 80 °C until it is completely dissolved, then filter it with a 0.22 μm filter and store it in a 50 mL centrifuge tube for measurement.[34]

2.7 Chromatographic conditions

Column was VP-ODS C_{18} Column (250 mm × 4.6 mm); mobile phase was acetonitrile -to-water volume ratio of 75 : 25; column temperature was 25 °C; injection volume was 25.0 μL; flow rate was 1.0 mL min^{-1}; UV detector detection wavelength was 484 nm.

3 Results and discussion

3.1 Characterization of Cu/Co-MOF@[PrPy][Br]

3.1.1 SEM and TEM. The surface morphologies of Cu/Co-MOF and Cu/Co-MOF@[PrPy][Br] were observed by SEM and TEM, and the scanning results were shown in Fig. 1. The comprehensive analysis showed that Cu/Co-MOF@[PrPy][Br] still maintained the three-dimensional framework of Cu/Co-MOF. And many pores were formed in Cu/Co-MOF when ionic liquids were mixed.

3.1.2 FT-IR. As shown in Fig. 2a, Fourier transform infrared spectra of Cu/Co-MOF, [PrPy][Br] and Cu/Co-MOF@[PrPy][Br] were recorded in the wave-number range of 4000–800 cm^{-1}. The peak at 1445 cm^{-1} in curve 1 corresponds to the –O–C–O– stretching vibration of homo-triformic acid, and the peaks at 1373 cm^{-1} and 1650 cm^{-1} corresponds to the stretching and bending vibration of Cu–O–H and Co–O–H respectively, proving that Cu/Co-MOF was successfully prepared.[35] In curve 2, the peak at 1635 cm^{-1} corresponds to the C=N stretching vibration on the pyridine ring, while the peaks at 2680 cm^{-1}, 2962 cm^{-1} and 3040 cm^{-1} were $-CH_3$, $-CH_2$ and C–H stretching vibration on the pyridine ring respectively. The characteristic peaks of Cu/Co-MOF@[PrPy][Br] correspond to Cu/Co-MOF and [PrPy][Br], and part of the characteristic peaks were offset, which could be attributed to the extension or shortening of the chemical bond

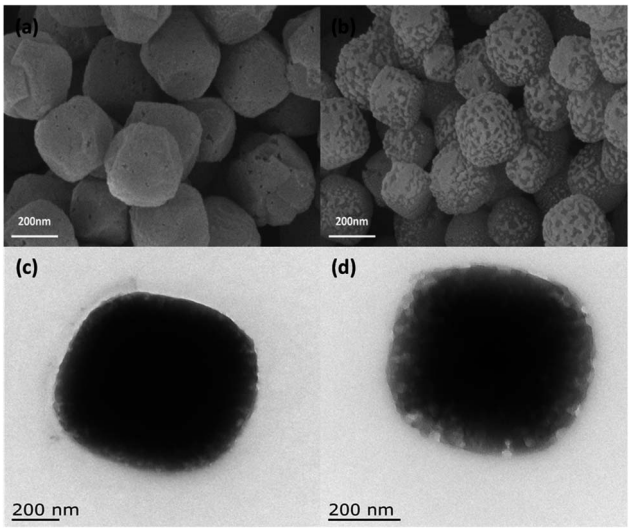

Fig. 1 SEM and TEM images of Cu/Co-MOF and Cu/Co-MOF@[PrPy][Br].

between the MOF metal cluster and the connecting molecule caused by the addition of ionic liquid. These data indicated that Cu/Co-MOF@[PrPy][Br] composites were successfully synthesized.

3.1.3 XRD. The XRD pattern was used to characterize the crystal structure of Cu/Co-MOF@[PrPy][Br] and the results were shown in Fig. 2b. Curves 1 and 2 were the spectra of Cu/Co-MOF and Cu/Co-MOF@[PrPy][Br] respectively. It could be seen from the Fig. 2b that with the incorporation of ionic liquid, the characteristic diffraction peaks of Cu/Co-MOF was no obvious change, indicating that the entry of ionic liquid did not affect the structural integrity of the Cu/Co-MOF, but the XRD band intensity of Cu/Co-MOF@[PrPy][Br] was lower than that of Cu/Co-MOF, indicating that the crystallinity of the composite was lower than that of the pristine MOF.

3.1.4 Zeta. The zeta potential of Cu/Co-MOF@[PrPy][Br] in the pH range of 4.0–10.0 was shown in Fig. 2c. It could be seen that the potential value of Cu/Co-MOF@[PrPy][Br] changed with the pH of the solution, and its surface was always negatively charged, which was a good site for cation and positively charged molecules to combine.

3.2 Optimization of extraction conditions

3.2.1 Types of extractants. The effects of four materials (Cu-MOF, Co-MOF, Cu/Co-MOF, Cu/Co-MOF@ [PrPy][Br]) on extraction efficiency of sunset yellow were studied. The results were shown in Fig. 3a. Compared with the other three materials, Cu/Co-MOF@[PrPy][Br] had better extraction performance due to the synergistic effect between the bimetals. Therefore, Cu/Co-MOF@[PrPy][Br] was selected as the best extractant.

3.2.2 Influence of extractant dosage. The amount of extractant in SPE directly affected the extraction efficiency. The effect of Cu/Co-MOF@[PrPy][Br] dosage in the range of 2.0–20.0 mg on extraction efficiency of sunset yellow was studied. As could be seen from Fig. 3b that the extraction of sunset yellow reached equilibrium when the dosage of extractant was 5.0 mg, Therefore, the optimal dosage of Cu/Co-MOF@[PrPy][Br] was 5.0 mg.

3.2.3 Effect of pH. The influence of pH value on extraction efficiency of sunset yellow was in the range of 3.0–10.0 (Fig. 3c). The extraction efficiency was higher than 90% in the range of pH 3.0–5.0, and gradually decreased in the range of 6.0–10.0. The pK_a of sunset yellow was 6.0,[36] which was protonated under acidic conditions. At the same time, according to zeta potential (Fig. 2c), Cu/Co-MOF@[PrPy][Br] had a negative charge on its surface, so the extraction efficiency was high. Under alkaline conditions, sunset yellow mainly existed in the form of anions, leading to the reduction of extraction efficiency.[37] Therefore, the optimal pH value was 5.0.

3.2.4 Effect of extraction time. The effect of extraction time on extraction efficiency was studied within 2–30 min. The results showed that the extraction efficiency of sunset yellow was more than 95.0% within 15 min and remained stable. So the optimal extraction time was 15 minutes.

3.2.5 Effect of extraction temperature. The influence of extraction temperature on extraction efficiency was investigated in the range of 0–40 °C. The results showed that the extraction efficiency of sunset yellow reached its maximum value at 25 °C and decreased slightly with the increase of temperature. Therefore, 25 °C was selected as the best experimental temperature.

3.2.6 Sample volume. The influence of sample volume on extraction efficiency was studied and the result was shown in Fig. 3d. With the increase of solution volume, the extraction

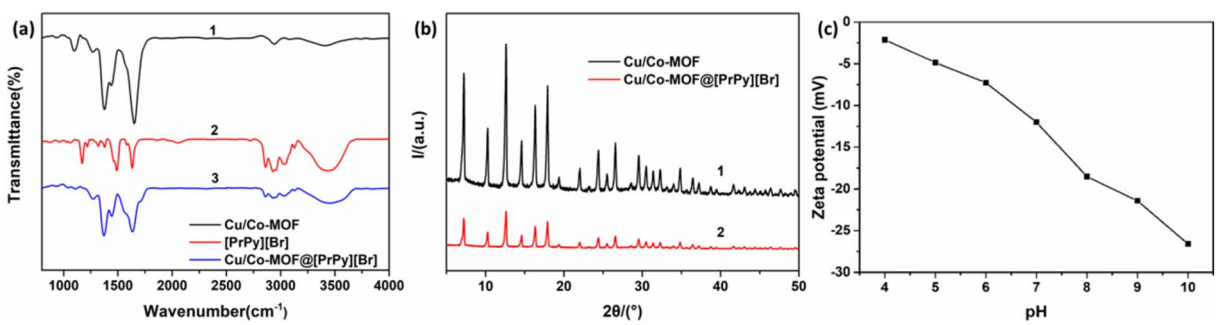

Fig. 2 (a) FT-IR spectra of Cu/Co-MOF, [PrPy][Br] and Cu/Co-MOF@[PrPy][Br]; (b) XRD pattern of Cu/Co-MOF and Cu/Co-MOF@[PrPy][Br]; (c) zeta potential of Cu/Co-MOF@[PrPy][Br].

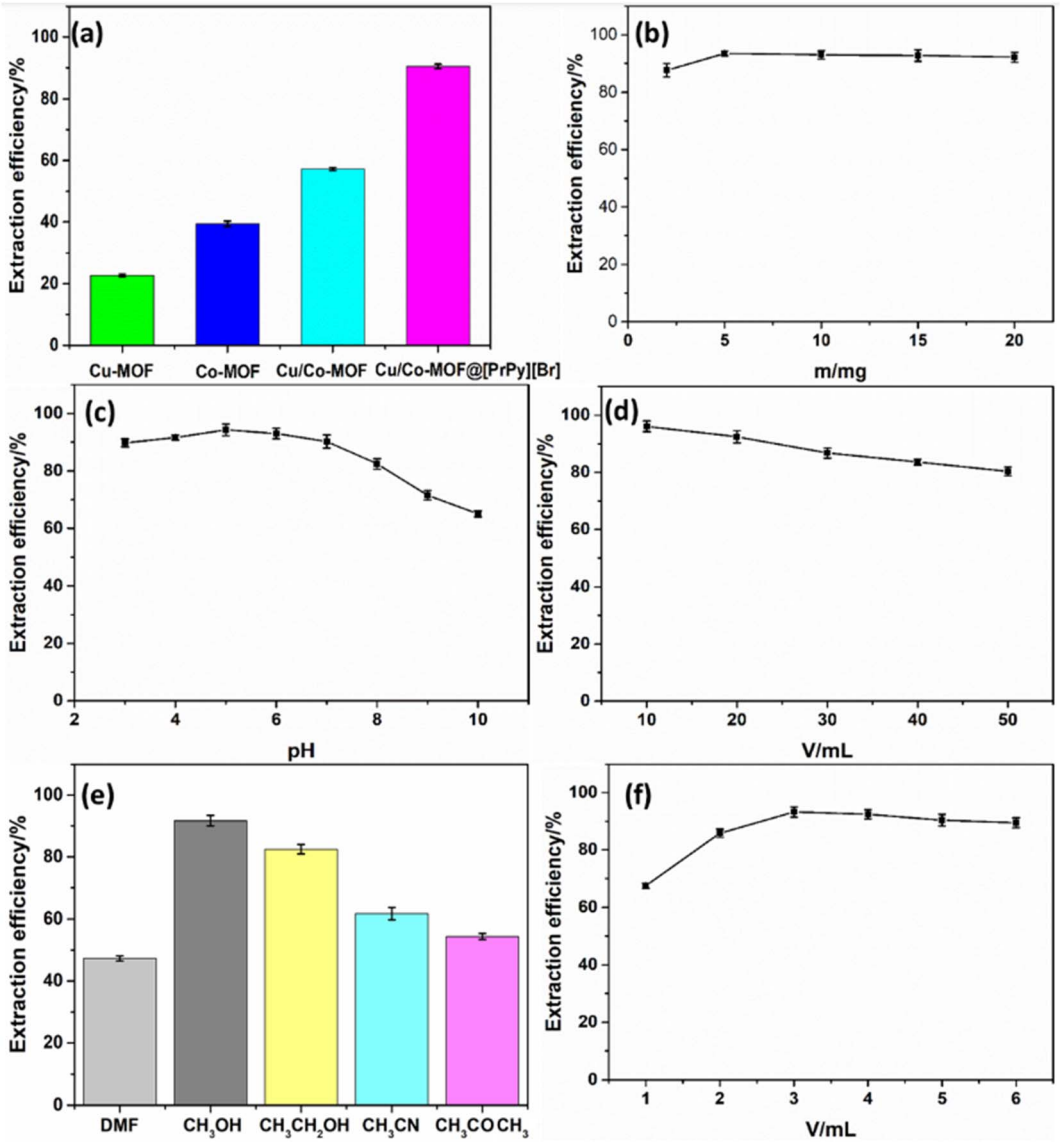

Fig. 3 Optimization of analysis conditions (1.0 μg mL^{-1} sunset yellow solution). Effect of (a) type of extractant, (b) extractant dosage, (c) pH, (d) sample volume, (e) eluents, (f) eluent volume.

efficiency of Cu/Co-MOF@[PrPy][Br] decreased continuously. When the volume of solution exceeded 30.00 mL, the extraction efficiency is lower than 85%. Therefore, the maximum allowable sample volume was 30.00 mL.

3.3 Optimization of elution conditions

3.3.1 Types of eluents. Sunset yellow was eluted from Cu/Co-MOF@[PrPy][Br] with a small amount of eluent to achieve separation and enrichment of sunset yellow. The elution effects of DMF, methanol, ethanol, acetonitrile and acetone were studied experimentally. As shown in Fig. 3e, methanol had the highest elution efficiency for sunset yellow. Therefore, methanol was selected as the eluent.

3.3.2 Effect of elution volume. The amount of eluent directly affects the elution efficiency. The effect of methanol dosage (1.00–6.00 mL) on elution efficiency was studied. As shown in Fig. 3f, the elution efficiency increased with the increasing of eluting volume. The maximum elution efficiency was achieved at 3.00 mL. Therefore, 3.00 mL was selected as the optimal elution volume. Sunset yellow was pre-enriched at 10 time (pre-extraction solution volume/elution volume).

3.3.3 Effect of elution time. The effect of elution time on elution efficiency was studied within 2–30 min. The results showed that the elution efficiency reached its maximum value within 10 minutes and then remained unchanged. Therefore, the optimal elution time was 10 minutes.

3.3.4 Effect of elution temperature. The influence of elution temperature on elution efficiency was investigated in the range of 0–40 °C. The results showed that the elution efficiency of sunset yellow reached its maximum value at 25 °C and remained stable with the increase of temperature. Therefore, 25 °C was chosen as the optimal elution temperature.

3.4 Reuse times

Considering the maximization of material utilization, Cu/Co-MOF@[PrPy][Br] was eluted under the optimal elution conditions after extraction. The result showed that after 5 times of extraction-elution, the extraction efficiency remained above 85%. The results showed that Cu/Co-MOF@[PrPy][Br] had good stability and reusability.

3.5 Interference experiment

The influence of interfering substances on the extraction efficiency of sunset yellow was studied. The allowable error range was ≤±5%. The results showed that when the concentration ratios of Rhodamine 6G, Sudan, lemon yellow, Allura Red, and methyl blue to sunset yellow were 100, 100, 5, 25, and 25 respectively, these interfering substances had no effect on the determination of sunset yellow.

3.6 Analysis application

Under the optimal conditions, the linear range of sunset yellow was 0.05–40.0 μg mL^{-1}. The linear equation was A (peak area) = $2.41 \times 10^6 c + 5.81 \times 10^4$ (μg mL^{-1}). The linear correlation coefficient (R^2) was 0.9992, detection limit was 0.02 μg mL^{-1}.

3.7 Sample analysis

The chromatograms of samples measured under optimal conditions was obtained. As shown in Fig. 4, curve a represented the chromatogram of sunset yellow standard solution, and curves b, c and d represented extraction of real sample spiked with sunset yellow standard solution, the real sample with and without extraction respectively. It could be seen from Fig. 4 that: (1) the retention time of sunset yellow was about 6.38 min; (2) the sunset yellow signal in the real sample was significantly enhanced after the extraction (curves b, c and d).

The real samples were determined by standard addition method. Table 1 showed that no sunset yellow was detected in soda, and the contents of sunset yellow in effervescent tablet and jelly were 0.051 and 0.062 μg g^{-1} respectively, which all met the Chinese national standard (GB 2760-2014). The recovery of sunset yellow in real samples ranged from 92.5% to 108.0%, which could be used for the determination of sunset yellow in real samples.

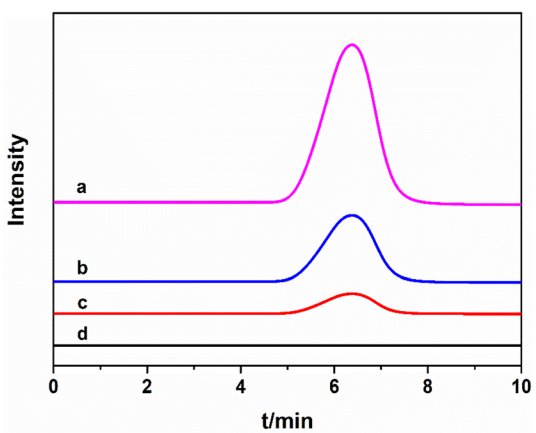

Fig. 4 HPLC chromatograms. (a) Sunset yellow standard solution; (b) extraction of real sample spiked with sunset yellow standard solution; (c) real sample after extraction; (d) real sample without extraction.

Table 1 Real sample analysis

Sample	Added value (mg L^{-1})	Measured value (mg L^{-1})	Recovery (%)
Soda	—	—	—
	0.500	0.514	102.8
	1.000	0.970	97.0
	2.000	1.850	92.5
Effervescent tablet	—	0.051	—
	0.500	0.487	97.4
	1.000	1.080	108.0
	2.000	1.910	95.5
Jelly	—	0.062	—
	0.500	0.508	101.6
	1.000	0.974	97.4
	2.000	1.980	99.0

3.8 Comparison of the proposed method with the reported methods

To further evaluate the performance of the present method, four previously reported methods for determining sunset yellow[38–41] in different matrices were compared with the present method and the detailed results are summarized in Table 2. The linear range and LOD were comparable to those in the previously reported methods, demonstrating the reliability of the proposed method. It should be pointed out that the parameters, such as enhancement factor, sample volume, LOD of this method have a superior performance, and the extractant can be reused.

3.9 Adsorption (extraction) mechanism studies

3.9.1 Adsorption kinetics. The adsorption mechanism of this experiment was explored by using pseudo first-order and pseudo second-order kinetic models at 20 °C, and the fitting equation was as follows:[42]

$$\text{Pseudo-first-order: } \ln(q_e - q_t) = \ln q_e - k_1 t$$

$$\text{Pseudo-second-order: } t/q_t = 1/k_2 q_e + t/q_e$$

where q_t (mg g^{-1}) is the adsorption amount at time t (min), q_e (mg g^{-1}) is the equilibrium adsorption amount, and k_1 and k_2 are the pseudo-first-order and pseudo-second-order adsorption rate constants.

The fitting curve were shown in Fig. 5a and b. It could be seen that the pseudo-second-order kinetic curve was better than the pseudo-first-order kinetic curve, and the linear correlation coefficient was 0.9987. Therefore, the pseudo-second-order kinetic model could better explain the adsorption process of sunset yellow of Cu/Co-MOF@[PrPy][Br], indicating that the process was chemical adsorption (extraction).

Table 2 Comparison of the proposed method with some reported methods for the enrichment and determination of sunset yellow

Methods	Samples	Enhancement factor	Linger range (μg L^{-1})	Extraction time (min)	Sample volume (mL)	LOD (μg L^{-1})	Ref.
SPE-HPLC	Sports drinks	1.5	—	20	2	50.0	38
SPE-UV	Beverage samples	4	100–10000	9	4	37.0	39
SPE-CE	Preserved fruit	5	100–50000	10	15	35.0	40
SPE-UV	Orange beverages, ice products, snacks, orange jelly powders	10	1000–120000	15	20	410	41
SPE-HPLC	Soda, effervescent tablet, jelly	10	50–40000	15	30	20.0	This work

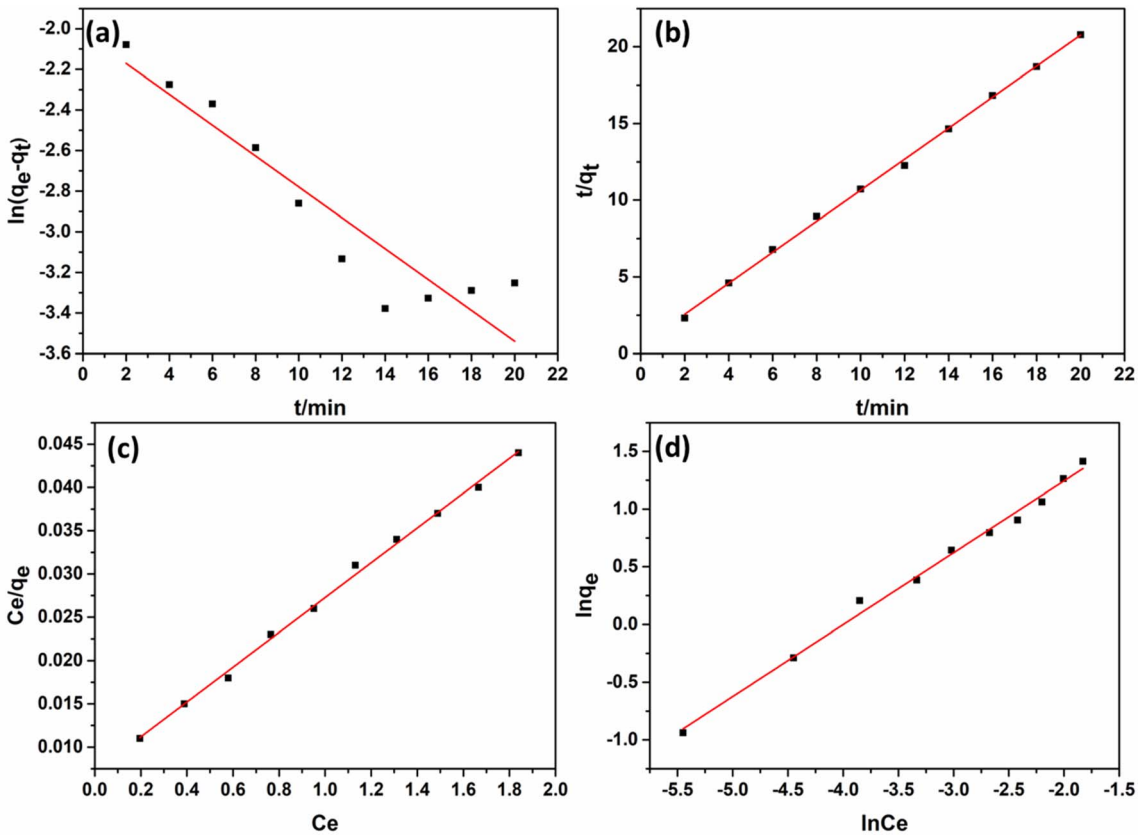

Fig. 5 (a) Pseudo-first-order and (b) pseudo-second-order adsorption kinetic model of sunset yellow; (c) Langmuir and (d) Freundlich adsorption isotherm of ZIF-8@MIM–MIM composite to sunset yellow.

3.9.2 Adsorption isotherm model. The adsorption isotherms of different initial concentrations of sunset yellow at 20 °C were studied and analyzed by the Langmuir and Freundlich adsorption isotherm model. The equation were as follows:[43]

$$\text{Langmuir equation: } C_e/q_e = C_e/q_{max} + 1/q_{max}K_L$$

$$\text{Freundlich equation: } \ln q_e = \ln C_e/n + \ln K_F$$

where q_e (mg g^{-1}) is the adsorption capacity at equilibrium, C_e (mg L^{-1}) is the equilibrium concentration, K_L and K_F are adsorption equilibrium constants, q_{max} (mg g^{-1}) is the maximum adsorption capacity.

The results were shown in Fig. 5c and d. The linear correlation coefficients of the Langmuir and Freundlich models are 0.9971 and 0.9927 respectively, so the Langmuir adsorption isotherm model was more suitable for the adsorption of sunset yellow on Cu/Co-MOF@[PrPy][Br]. The monolayer adsorption capacity calculated from the Langmuir isotherm was 50.00 mg g^{-1}.

4 Conclusion

In this work, bisimidazole ionic liquid-functionalized metal organic framework composite (Cu/Co-MOF@[PrPy][Br]) was prepared and used as solid-phase extractant coupled with high

performance liquid chromatography for the separation and analysis of sunset yellow in food. Compared with monometallic MOF, the bimetallic in Cu/Co-MOF@[PrPy][Br] endow the composites with more tunable active sites, due to the synergistic effect between the bimetals and has better recycling performance. The method is applied to the analysis of real samples with feasible, economical and practical, and the analytical results are satisfactory.

Conflicts of interest

All authors declare there is no conflicts of interest.

Acknowledgements

The authors acknowledge the financial support from the National Natural Science Foundation of China (21375117) and a project funded by the Priority Academic Program Development of Jiangsu Higher Education Institutions.

References

1 T. Gan, J. Sun, W. Meng, L. Song and Y. X. Zhang, Electrochemical sensor based on graphene and mesoporous TiO_2 for the simultaneous determination of trace colourants in food, *Food Chem.*, 2013, **141**(4), 3731–3737.

2 S. A. R. Hosseininia, M. H. Kamani and S. Rani, Quantitative determination of sunset yellow concentration in soft drinks via digital image processing, *J. Food Meas. Char.*, 2017, **11**(3), 1065–1070.

3 W. Zhang, T. Liu, X. Zheng, W. S. Huang and C. D. Wan, Surface-enhanced oxidation and detection of Sunset Yellow and Tartrazine using multi-walled carbon nanotubes film-modified electrode, *Colloids Surf., B*, 2009, **74**(1), 28–31.

4 L. Ji, Q. Cheng, K. Wu and X. F. Yang, Cu-BTC frameworks-based electrochemical sensing platform for rapid and simple determination of Sunset yellow and Tartrazine, *Sens. Actuators, B*, 2016, **231**, 12–17.

5 Y. E. Unsal, M. Soylak and M. Tuzen, Column solid-phase extraction of sunset yellow and spectrophotometric determination of its use in powdered beverage and confectionery products, *Int. J. Food Sci. Technol.*, 2012, **47**(6), 1253–1258.

6 D. Ş. Zor, B. Aşçı and A. Ö. Dönmez, Simultaneous Determination of Potassium Sorbate, Sodium Benzoate, Quinoline Yellow and Sunset Yellow in Lemonades and Lemon Sauces by HPLC Using Experimental Design, *J. Chromatogr. Sci.*, 2016, **54**(6), 952–957.

7 K. Zhang, P. Luo, J. Wu, W. Wang and B. Ye, Highly sensitive determination of Sunset Yellow in drink using a poly (l-cysteine) modified glassy carbon electrode, *Anal. Methods*, 2013, **5**(19), 5044–5050.

8 Y. Yuan, X. Zhao, M. Qiao, J. H. Zhu, S. P. Liu, J. D. Yang and X. L. Hu, Determination of sunset yellow in soft drinks based on fluorescence quenching of carbon dots, *Spectrochim. Acta, Part A*, 2016, **167**, 106–110.

9 W. A. Khan, M. B. Arain and M. Soylak, Nanomaterials-based solid phase extraction and solid phase microextraction for heavy metals food toxicity, *Food Chem. Toxicol.*, 2020, **145**, 111704.

10 J. S. Pyo, H. S. Lee and J.-H. Kwak, Determination of Gamma-Hydroxybutyric Acid in Urine by Solid Phase Extraction and Gas Chromatography-Mass Spectrometry, *Anal. Lett.*, 2016, **49**(2), 217–225.

11 H. Braus, F. Middleton and G. Walton, Orangic Chemical Compounds in Raw and Filtered Surface Waters, *Anal. Chem.*, 1951, **23**(8), 1160–1164.

12 K. Pyrzyñska and Z. Joñca, Multielement Preconcentration and Removal of Trace Metals by Solid-Phase Extraction, *Anal. Lett.*, 2000, **33**(7), 1441–1450.

13 A. L. de Toffoli, E. V. S. Maciel and B. H. Fumes, The role of graphene-based sorbents in modern sample preparation techniques, *J. Sep. Sci.*, 2018, **41**(1), 288–302.

14 N. Manousi, D. A. Giannakoudakis and E. Rosenberg, Extraction of Metal Ions with Metal-Organic Frameworks, *Molecules*, 2019, **24**(24), 4605.

15 Y. Ma, Y. Ruan and X. Gao, Preparation of a Novel Resin Based Covalent Framework Material and Its Application in the Determination of Phenolic Endocrine Disruptors in Beverages by SPE-HPLC, *Polymers*, 2021, **13**(17), 2935.

16 Z.-L. Wu, Q. Liu, X.-Q. Chen and J. G. Yu, Preconcentration and analysis of Rhodamine B in water and red wine samples by using magnesium hydroxide/carbon nanotube composites as a solid-phase extractant, *J. Sep. Sci.*, 2015, **38**(19), 3404–3411.

17 J. P. Chen and X. S. Zhu, Ionic liquid coated magnetic core/shell Fe_3O_4@SiO_2 nanoparticles for the separation/analysis of linuron in food samples, *Spectrochim. Acta, Part A*, 2015, **137**, 456–462.

18 J.-Y. Chen, S.-R. Cao, C.-X. Xi and Y. Chen, ZQ Chen A novel magnetic β-cyclodextrin modified graphene oxide adsorbent with high recognition capability for 5 plant growth regulators, *Food Chem.*, 2018, **239**, 911–919.

19 X. Wei, Y. Wang, J. Chen, P. Xu and Y. G. Zhou, Preparation of ionic liquid modified magnetic metal-organic frameworks composites for the solid-phase extraction of α-chymotrypsin, *Talanta*, 2018, **182**, 484–491.

20 M. A. Habila, B. Alhenaki, A. El-Marghany, M. Sheikh, A. A. Ghfar, Z. A. ALOthman and M. Soylak, Metal Organic Framework-Based Dispersive Solid-Phase Microextraction of Carbaryl from Food and Water Prior to Detection by Ultra-Performance Liquid Chromatography-Tandem Mass Spectrometry, *J. Sep. Sci.*, 2020, **43**, 3103–3109.

21 S. Bourrelly, P. L. Llewellyn and C. Serre, Different Adsorption Behaviors of Methane and Carbon Dioxide in the Isotypic Nanoporous Metal Terephthalates MIL-53 and MIL-47, *J. Am. Chem. Soc.*, 2005, **127**(39), 13519–13521.

22 J. L. C. Rowsell and O. M. Yaghi, Metal–organic frameworks: a new class of porous materials, *Microporous Mesoporous Mater.*, 2004, **73**(1), 3–14.

23 Y. Shen, Z. Li and L. Wang, Cobalt-citrate framework armored with graphene oxide exhibiting improved thermal

stability and selectivity for biogas decarburization, *J. Mater. Chem. A*, 2015, **3**(2), 593–599.

24 P. Thangavel, M. Ha and S. Kumaraguru, Graphene-nanoplatelets-supported NiFe-MOF: high-efficiency and ultra-stable oxygen electrodes for sustained alkaline anion exchange membrane water electrolysis, *Energy Environ. Sci.*, 2020, **13**(10), 3447–3458.

25 A. Jarrah and S. Farhadi, Preparation and characterization of novel polyoxometalate/$CoFe_2O_4$/metal–organic framework magnetic core-shell nanocomposites for the rapid removal of organic dyes from water, *RSC Adv.*, 2020, **10**(65), 39881–39893.

26 S. Zheng, J. Hu and X. Cui, In situ Growth of a Cobalt-based Metal-organic Framework on Multi-walled Carbon Nanotubes for Simultaneously Detection of Hydroquinone and Catechol, *Electroanalysis*, 2020, **32**(9), 2010–2017.

27 L. Huang, W. Huang, R. Shen and S. A. Qin, Chitosan/thiol functionalized metal-organic framework composite for the simultaneous determination of lead and cadmium ions in food samples, *Food Chem.*, 2020, **330**, 127212.

28 A. Yohannes, X. Feng and S. Yao, Dispersive solid-phase extraction of racemic drugs using chiral ionic liquid-metal-organic framework composite sorbent, *J. Chromatogr. A*, 2020, **1627**, 461395.

29 J.-H. Qin, Y.-D. Huang, M.-Y. Shi, H.-R. Wang, M. L. Han, X. G. Yang, F. F. Li and L. F. Ma, Aqueous-phase detection of antibiotics and nitroaromatic explosives by an alkali-resistant Zn-MOF directed by an ionic liquid, *RSC Adv.*, 2020, **10**(3), 1439–1446.

30 M. Sarker, I. Ahmed and S. H. Jhung, Adsorptive removal of herbicides from water over nitrogen-doped carbon obtained from ionic liquid@ZIF-8, *Chem. Eng. J.*, 2017, **323**, 203–211.

31 H. Ji, K. Naveen and W. Lee, Pyridinium-Functionalized Ionic Metal-Organic Frameworks Designed as Bifunctional Catalysts for CO_2 Fixation into Cyclic Carbonates, *ACS Appl. Mater. Interfaces*, 2020, **12**(22), 24868–24876.

32 F. Tian, C. Qiao, R. Zheng, R. Y. Zheng, Q. F. Ru, X. Sun, Y. F. Zhan and C. G. Meng, Synthesis of bimetallic-organic framework Cu/Co-BTC and the improved performance of thiophene adsorption, *RSC Adv.*, 2019, **9**(27), 15642–15647.

33 Z. Guo, W. Zheng, X. Yan, D. Yan, X. H. Ruan, X. H. Yang, X. C. Li, N. Zhang and G. H. He, Ionic liquid tuning nanocage size of MOFs through a two-step adsorption/infiltration strategy for enhanced gas screening of mixed-matrix membranes, *J. Membr. Sci.*, 2020, **605**, 118101–118109.

34 Z. Lotfi, H. Mousavi and M. S. Sajjadi, A hyperbranched polyamidoamine dendrimer grafted onto magnetized graphene oxide as a sorbent for the extraction of synthetic dyes from foodstuff, *Microchim. Acta*, 2017, **184**(11), 4503–4512.

35 J. Zhang, C. Zhang and X. Duo, Self-assembled acicular CuCo-MOF for enhancing oxygen evolution reaction, *Ionics*, 2020, **26**(10), 5123–5132.

36 M. Kamalabadi, M. M. Razavi-Mashouf and T. Madrakian, Electrochemically controlled solid phase microextraction based on nanostructured polypyrrole film for selective extraction of sunset yellow in food samples, *J. Iran. Chem. Soc.*, 2021, **18**(11), 3127–3135.

37 R. Khani and M. Irani, Mixed Magnetic Dispersive Micro-Solid Phase-Cloud Point Extraction of Sunset Yellow in Food and Pharmaceutical Samples, *ChemistrySelect*, 2021, **6**(3), 273–278.

38 L. Floriano, L. C. Ribeiro, N. Saibt, N. M. G. Bandeira, O. D. Prestes and R. Zanella, Determination of Six Synthetic Dyes in Sports Drinks by Dispersive Solid-Phase Extraction and HPLC-UV-Vis, *Soc. Bras. Quim.*, 2018, **29**, 602–608.

39 W. J. Li, Q. Jia, Z. Y. Zhang and Y. P. Wang, Preparation of γ-alumina nanoparticle modified polyacrylamide composite and study on its solid phase extraction of Sunset Yellow, *Korean J. Chem. Eng.*, 2016, **33**, 1337–1344.

40 J. Yi, L. Zeng and Q. Wu, Sensitive Simultaneous Determination of Synthetic Food Colorants in Preserved Fruit Samples by Capillary Electrophoresis with Contactless Conductivity Detection, *Food Anal. Methods*, 2018, **11**(6), 1608–1618.

41 B. Hatamluyi, R. Sadeghian, F. Malek and M. T. Boroushaki, Improved solid phase extraction for selective and efficient quantification of sunset yellow in different food samples using a novel molecularly imprinted polymer reinforced by Fe_3O_4@UiO-66-NH_2, *Food Chem.*, 2021, **357**, 129782–129789.

42 T. A. Saleh, A. Sarı and M. Tuzen, Effective adsorption of antimony(III) from aqueous solutions by polyamide-graphene composite as a novel adsorbent, *Chem. Eng. J.*, 2017, **307**, 230–238.

43 J. Fu, Z. Chen and M. Wang, Adsorption of methylene blue by a high-efficiency adsorbent (polydopamine microspheres): Kinetics, isotherm, thermodynamics and mechanism analysis, *Chem. Eng. J.*, 2015, **259**, 53–61.